The Journal of Engineering

The 9th International Conference on Power Electronics, Machines and Drives (PEMD 2018)

The Institution of Engineering and Technology Journals

Evaluating suitable semiconducting materials for cryogenic power electronics

eISSN 2051-3305
Received on 22nd June 2018
Accepted on 27th July 2018
E-First on 4th April 2019
doi: 10.1049/joe.2018.8099
www.ietdl.org

Luke Bradley[1] ✉, Christopher Donaghy-Spargo[2], Glynn Atkinson[1], Alton Horsfall[1]
[1]Department of Emerging Technologies and Materials, School of Engineering, Newcastle University, Newcastle, NE1 7RU, UK
[2]Department of Engineering, School of Engineering, University of Durham, Durham, DH1 3LE, UK
✉ E-mail: l.j.bradley@newcastle.ac.uk

Abstract: The interest in hybrid electric aircraft has invigorated research into superconducting power networks and superconducting electrical machines. Underpinning this is the ability to control the flow of electrical current at cryogenic temperatures, using power electronic devices. The authors have, for the first time, directly compared the performance of technologically relevant semiconductor materials for the realisation of high-performance cryogenic power devices using a bulk resistivity model. By validating the model using both computational and experimental results, the performance of technologically relevant semiconductors has been calculated down to a temperature of 20 K where the freeze out of dopants is shown to be the major limiting factor in determining the performance of power electronic devices. Both Ge and GaAs are predicted to have a superior conductivity in comparison to the industrial standards Si and 4H-SiC due to greater carrier mobilities and lower dopant ionisation energies.

1 Introduction

A number of applications are examining the possibility of using superconducting cables for the transfer of electrical power, including power distribution networks and more recently the concept of developing hybrid electric propulsion systems for aircraft [1, 2]. This is being driven by ongoing research to identify more efficient designs for air travel, which are being pursued by organisations including the national aeronautics and space administration (NASA) and aerospace technical institute. The ability to operate a large number of distributed electrical machines is a critical aspect of the aircraft design and this is only practical using a superconducting power network. In order to provide control over the behaviour of the machine and provide isolation in the case of failure, an integrated control circuit consisting of high power electronic devices that can operate while cooled by liquid hydrogen is required.

To meet the requirements of the design proposed by NASA [2], the semiconductor selected needs to demonstrate

i. Low on-state resistance at 20 K
ii. Low resistance variation with temperature around 20 K

As the optimum transistor topology is not known at this nascent stage of the research, losses during the switching of the power electronic circuit have not been considered, as the transient behaviour of the transistors is critically dependent on both the selected topology and the circuit environment in which it will be used.

In power devices, it is known that the overall resistance of a device is the sum of multiple regions and other resistances such as channel resistance, accumulation resistance, spreading resistance and contact resistances [3–7]. Here, these resistances have not been taken into account. The assumption in this work is that the resistive contributions from the lightly doped drift layer of vertical devices are sufficient that other resistive contributions can be safely ignored and this will be validated using experimental and computation results for a vertical PiN diode structure at multiple temperatures down to 20 K.

The aim of this work is to compare the cryogenic performance devices fabricated from the industrial standards Si and 4H-SiC to lesser used materials Ge and GaAs in order to determine which material would be most suited for cryogenic power electronic devices.

2 Material properties

The physical parameters of the semiconductors studied here, including permittivity and the density of states effective mass, were taken from reference [8] and the ionisation energies of dopants in Ge, Si, GaAs and 4H-SiC were taken from references [9–11]. The specific on state resistance of an n-type power device can be expressed as

$$R_{\text{on-sp}} = \frac{L_{\text{drift}}}{ne\mu_n} \tag{1}$$

where L_{drift} is the length of the drift region, n is the free electron concentration, e is the electronic charge and μ_n is the electron drift mobility.

To simulate the electron mobility for temperatures between 20 and 300 K, polynomial functions were used to fit experimentally measured data from references [10, 12–14] resulting in the solid lines shown in Fig. 1*a*. Using Boltzmann statistics, the free electron concentration in an n-type semiconductor is given by

$$n = N_{\text{C}}\exp\left(-\frac{E_{\text{C}} - E_{\text{F}}}{k_{\text{B}}T}\right) \tag{2}$$

where N_{C} is the density of states in the conduction band, E_{C}–E_{F} is the difference between conduction band and Fermi energy level and $k_{\text{B}}T$ is the thermal energy. The concentration of thermally ionised donors can be modelled using [11]

$$N_{\text{D}}^{+} = \frac{N_{\text{D}}}{1 + \vartheta_{\text{D}}\exp\left(\frac{E_{\text{F}} - E_{\text{D}}}{k_{\text{B}}T}\right)} \tag{3}$$

where N_{D} is the donor concentration, ϑ_{D} is the electron degeneracy and E_{D} the energy of the dopant below the conduction band edge. The calculations are based on nitrogen in 4H-SiC ($E_{\text{D}} = 59$ meV [15]), antimony in both silicon ($E_{\text{D}} = 43$ meV [11]) and germanium

This is an open access article published by the IET under the Creative Commons Attribution License
(http://creativecommons.org/licenses/by/3.0/)

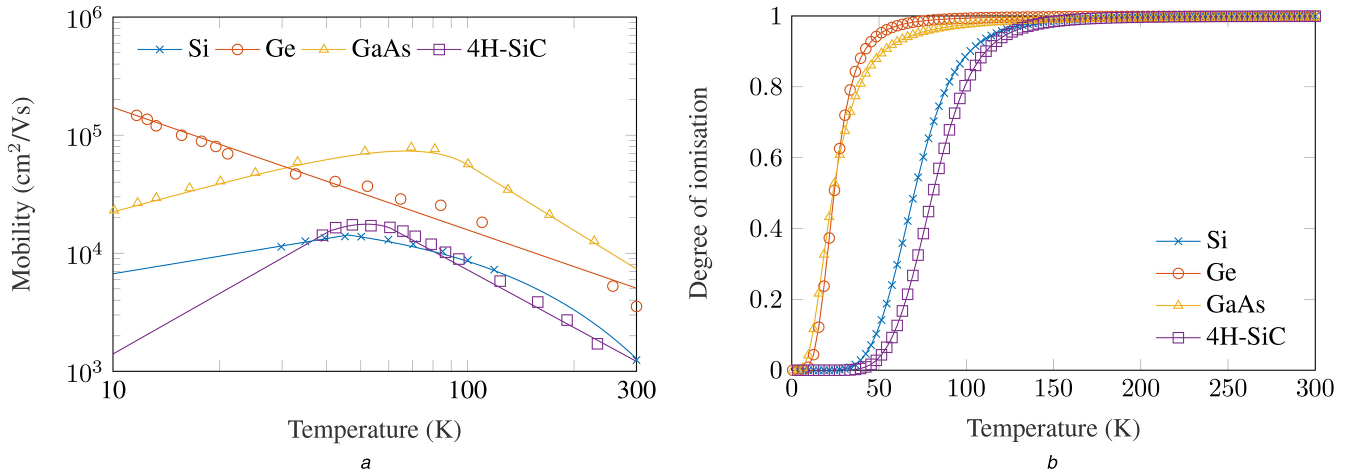

Fig. 1 *Experimental mobility and theoretical degree of ionisation (symbols) in bulk n-type Ge, Si, GaAs and 4H-SiC samples with dopant concentrations close to 10^{15} cm^{-3}. Values used for E_D are 43 meV for Si, 10 meV for Ge, 5:8 meV for GaAs and 59 meV for 4H-SiC*
(a) N-type mobility, ***(b)*** Degree of ionisation

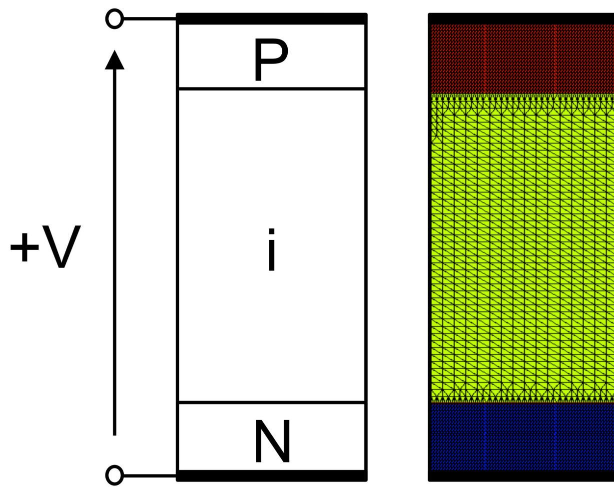

Fig. 2 *PiN structure used to simulate IV characteristics at cryogenic temperatures. Doping concentrations for contacts are 10^{20} cm^{-3} and ND = 10^{15}cm^{-3} for the lightly doped drift region denoted 'i'*

(E_D = 10 meV [9]) and silicon in gallium arsenide (E_D = 5.8 meV [11]).

The semiconductors considered here were analysed at cryogenic temperatures where the concentration of ionised donors is significantly greater than the intrinsic carrier concentration [11, 16]. As such, (2) and (3) can be equated and the free electron concentration can be expressed as a function of temperature for a given dopant concentration as shown in Fig. 1*b*.

2.1 TCAD simulation

The closed-loop equations provided in the previous subsection may model each individual component of a device theoretically, but that is not to say that a combination of all of these effects may lead to unexpected characteristics at cryogenic temperatures.

In order to validate the bulk resistivity model, technology computer-aided design (TCAD) was used to simulate a vertical PiN diode structure at multiple temperatures from 300 down to 20 K. TCAD simulations are performed by first defining a device with a 2D mesh as shown in Fig. 2, which is then used to calculate the current density $\boldsymbol{J} = \boldsymbol{J}_n + \boldsymbol{J}_p$ to satisfy the continuity equations

$$\nabla \cdot \boldsymbol{J}_n = eR_{\text{net}} + e\frac{\partial n}{\partial t} \tag{4a}$$

$$-\nabla \cdot \boldsymbol{J}_n = eR_{\text{net}} + e\frac{\partial n}{\partial t} \tag{4b}$$

where t is time and R_{net} is the net recombination rate given by the Shockley–Read–Hall formula [17–19]

$$R_{\text{net}} = \frac{np - n_{i,\text{eff}}^2}{\tau_p(n + n_1) + \tau_n(p + p_1)} \tag{5}$$

where $n_{i,\text{eff}}$ is the effective intrinsic carrier concentrations, τ_n and τ_p are the minority carrier lifetimes and n_1 and p_1 are given by

$$n_1 = n_{i,\text{eff}}\exp\left(\frac{E_{\text{trap}}}{k_B T}\right) \tag{6a}$$

$$p_1 = n_{i,\text{eff}}\exp\left(\frac{-E_{\text{trap}}}{k_B T}\right) \tag{6b}$$

where E_{trap} is the energy level of traps within the band gap which act as recombination centres. It will be shown later that the recombination must be considered when modelling bipolar devices based on minority carrier characteristics.

3 Results and discussion

3.1 Specific on-state resistance

The specific on state resistance of Si, Ge, GaAs and 4H-SiC is plotted in Fig. 3 based on the bulk resistivity model (1). For all materials, there are two distinct regions of operation. At higher temperatures where the majority of carriers are ionised, the resistance of all materials is dominated by optical phonon scattering which is not doping dependent for low doping concentrations [20].

At lower temperatures, the combined effects of carrier freeze out and ionised impurity scattering leads to an exponential increase in material resistivity. The specific on-state resistance of Ge and GaAs shows little difference at temperatures below 10 K as the majority of carriers freeze out at a similar rate as shown in Fig. 1*b*. Unlike Ge and GaAs, the effects of carrier freeze-out begin to dominate the specific on state resistance in Si and 4H-SiC below 60 K, which is due to the higher ionisation energies of antimony in Si (43 meV) and nitrogen in 4H-SiC (59 meV) and is the cause of the observed reduction in device performance that has been previously reported [5, 21, 22].

Reports comment on the exponential increase in resistance at cryogenic temperatures for power devices fabricated from Si and 4H-SiC, which is caused by a reduction of thermal energy required to ionise dopants. At higher doping concentrations, the ionisation energy of dopants reduces and the effective ionisation energy is given by

$$E_{\text{D,eff}} = E_{\text{D}} - \alpha_{\text{D}} N_{\text{tot}}^{1/3} \tag{7}$$

This is an open access article published by the IET under the Creative Commons Attribution License
(http://creativecommons.org/licenses/by/3.0/)

where E_D is the low doping concentration ionisation energy, α_D is a fitting parameter and N_{tot} is the total net doping concentration. Equation (7) has been used to model ionisation energy reduction for all the materials considered here [12, 23–28] although this effect only becomes appreciable for doping concentrations $>10^{17}$ cm^{-3} and so high doping levels cannot be used to improve the conductivity of power devices which require lightly doped drift regions of the order of 10^{14}–10^{15} cm^{-3}.

3.2 Model comparison to computational and experimental results

A comparison of the bulk resistivity model to computational TCAD and experimental results is plotted in Fig. 4. The Si PiN diode was simulated under three different conditions. The first simulation was used in order to validate the temperature dependence of the N-type drift region predicted by (1).

Following this, the Si PiN structure shown in Fig. 2 was simulated with and without Shockley–Read–Hall recombination current mechanism to see how this would affect device characteristics.

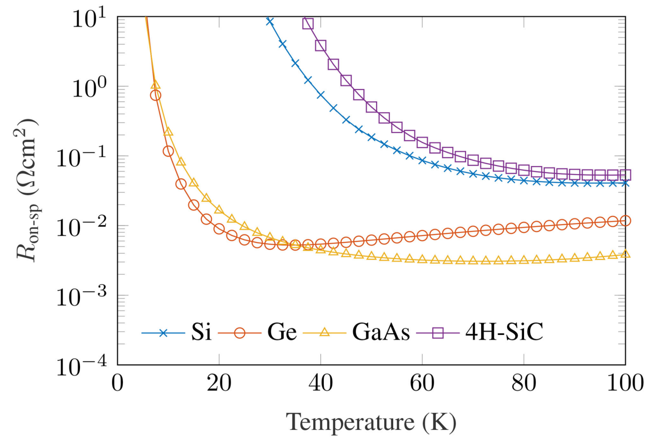

Fig. 3 *Specific on state resistance of N-type Si, Ge, GaAs and 4H-SiC for dopant concentrations of 10^{15} for a drift region length of 500 μm*

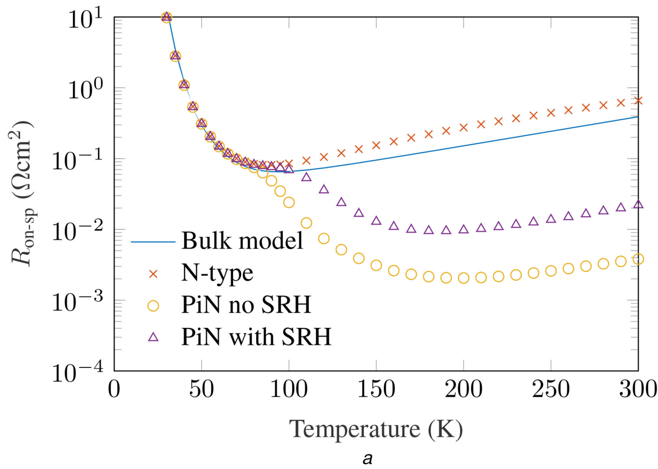

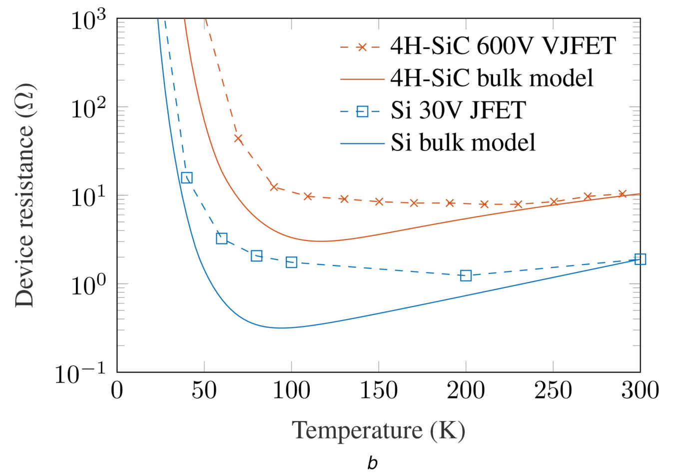

Fig. 4 *Comparison of the bulk resistivity model compared with the TCAD Si VJFET results (left) and experimental power JFET results*
(a) Bulk resistivity model comparison TCAD simulation results for the Si PiN diode with drift length of 500 μm, ***(b)*** Bulk resistivity model comparison to experimental results of a Si lateral JFET [29] and a 4H-SiC vertical JFET [21]

At all temperatures above 100 K, it can be seen that the resistance of the PiN diode cannot be simply modelled solely from the resistance of the drift as contributions from the P region and Shockley-Read-Hall (SRH) recombination mechanism reduce the PiN diode resistance at all temperatures. The generation and recombination rates for Si PiN diodes have been measured and modelled in the literature [19, 30–32] and must be considered when simulating bipolar devices. Although SRH mechanisms have not been considered in (1), the resistance of the PiN diode is accurately modelled at all temperatures below 100 K as the resistance of the device is dominated by carrier freeze out.

In order to validate the model presented here for industrial applications, the calculated data for Si and 4H-SiC in Fig. 3 is compared to measured data for a lateral Si JFET from [29] and a vertical 4H-SiC JFET from [21] and is plotted in Fig. 4*b*. The initial model predicts Si and 4H-SiC to have a much lower resistance compared to the measured data at temperatures between 70 and 200 K. The carrier freeze out regime is modelled well for Si whereas for 4H-SiC it can be seen that the carriers begin to freeze out a higher temperature than predicted. Correction for the carrier freeze out region of the 4H-SiC can be performed by considering that, unlike dopants in the other semiconductors considered here, 4H-SiC has two ionisation energies for nitrogen which are 59 meV (*k*-site) and 102 meV (*h*-site) [10, 33]. Of the two donor sites, the *k*-site is more preferable as carriers require less thermal energy to be ionised allowing for 4H-SiC devices to operate at lower temperatures although in reality there is an average of the two ionisation energies due to the positions of donors in lattice. As shown in Fig. 5, taking an average of the two ionisation energies improves the fit in the carrier freeze-out region of 4H-SiC in comparison to experimental data.

In the intermediate temperature range, further research shows that the exclusion of neutral impurity scattering has lead to a large disagreement in our model and experimental results [33–39]. The mobility data shown in Fig. 1*a* is taken from lateral measurements on wafers that were not used for devices. During device fabrication processes, P-regions are implanted into the wafer at high temperatures. During the high temperature anneal, it is possible for any residual oxide on the surface of wafers to become implanted and diffuse into the wafers leading to a concentration of unintentional impurities.

Unintentional impurities act as dopants with high ionisation energies. For example, oxygen impurities in samples act as donors with deep ionisation levels (0.061–0.51 eV in Si [11] and 0.175–0.185 eV in 4H-SiC [40]) and so are unionised at cryogenic temperatures resulting in a concentration of neutral impurities. The scattering rate from neutral impurities (N_{neu}) is given by [33, 38, 39]

$$\tau_{neu}^{-1} = \frac{80\pi\varepsilon_S N_{neu}\hbar^3}{(m_{e,dos}\, e)^2} \quad (8)$$

and is related to the carrier mobility by [11]

$$\mu = \frac{e\tau}{m_{e,cond}} \quad (9)$$

where $\hbar$ is the reduced Planck's constant, $m_{e,dos}$ is the electron density of states effective mass, τ is the average scattering rate and

This is an open access article published by the IET under the Creative Commons Attribution License
(http://creativecommons.org/licenses/by/3.0/)

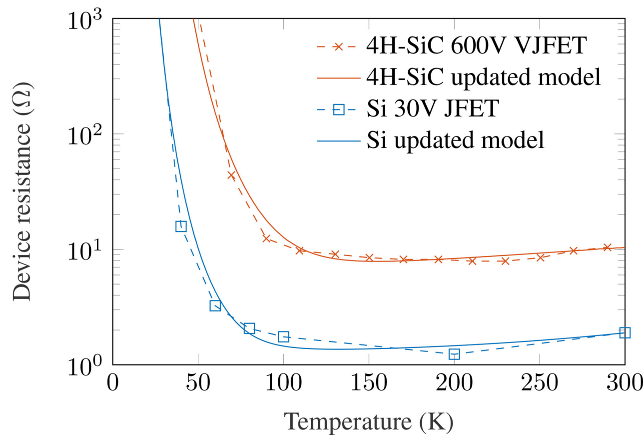

Fig. 5 *Updated model to take into consideration additional scattering mechanisms at intermediate temperatures*

$m_{e,\text{cond}}$ is the electron conductivity effective mass. For devices containing neutral impurities, the scattering rate given by (8) will result in a constant mobility at intermediate temperatures.

Modifying the mobility data in Fig. 1*a* to include scattering from neutral impurities improves the fitting in the intermediate temperature range for concentrations of 8×10^{17} in Si and 3 × 1018 cm^{-3} in 4H-SiC which is close to reported values for oxygen impurities in materials following annealing processes [41–43]. For 4H-SiC, this value is still high for devices with low dopant concentrations. Further research has suggested that the additional scattering in devices may occur from other mechanisms that are remnant from the fabrication process such as dislocation scattering and defect scattering. Despite this, the bulk mobility model is still able to accurately predict the performance of devices at cryogenic temperatures highlighting the limitations of Si and 4H-SiC for cryogenic power electronic applications.

4 Conclusion

The data show that Ge and GaAs are suitable candidates for cryogenic devices function in liquid hydrogen environments enabling a step change in capability for the aerospace industry. Analysis of the conductivity indicates that Ge has the best conductivity of the four semiconductors considered for temperatures below 37 K at a dopant concentration of 10^{15} cm^{-3}. This dopant concentration is typical of those used to form the drift region in power semiconductor devices and ensures the material retains high carrier mobility.

Analysis into the temperature dependence of the specific on state resistances shows that Ge and GaAs have values that are comparable to that of room-temperature devices. Corrections to the model to take into account scattering from neutral impurities and multiple donor energies allowed for experiment data of Si and 4H-SiC to be modelled and are deemed to be technologically unsuitable for cryogenic power applications as the high donor ionisation energies and considerable levels of ionised impurity scattering result in a material conductivity which is over 3 orders of magnitude smaller than that of either Ge or GaAs.

5 Acknowledgments

This work was supported by the Engineering and Physical Sciences Research Council (EPSRC) UK as part of the Advanced Aerospace Research Centre and the award of a PhD studentship through the Doctoral Training Grant scheme.

6 References

[1] Kim, H., Berton, J., Jones, S.: ‘Low noise cruise efficient short take-off and landing transport vehicle study’. 6th AIAA Aviation Technology, Integration and Operations Conference (ATIO), Reston, Virigina, February 2006, pp. 1–11

[2] Liu, C.: ‘Turboelectric distributed propulsion system modelling’, PhD thesis, Cranfield University, 2013

[3] Singh, R., Baliga, B.J.: ‘Power MOSFET analysis/optimization for cryogenic operation including the effect of degradation in breakdown voltage’. Proc. of the 4th Int. Symp. on Power Semiconductor Devices and Ics, 1992, pp. 339–344

[4] Singh, R., Baliga, B.J.: ‘Cryogenic operation of power junction field effect transistors’, *Solid-State Electron.*, 1996, **39**, (6), pp. 821–826

[5] Leong, K.: ‘Utilising Power Devices Below 100 K to Achieve Ultra-Low Power Losses’, PhD thesis, University of Warwick, 2011

[6] Kuzum, D., Krishnamohan, T., Nainani, A., *et al.*: ‘High-mobility Ge N-MOSFETs and mobility degradation mechanisms’, *IEEE Trans. Electron Devices*, 2011, **58**, (1), pp. 59–66

[7] Gallacher, K., Velha, P., Paul, D.J., *et al.*: ‘Ohmic contacts to n-type germanium with low specific contact resistivity’, *Appl. Phys. Lett.*, 2012, **100**, (2), p. 022113

[8] Levinshtein, M., Rumyantsev, S., Shur, M.: ‘*Handbook series on semiconductor parameters*’ (World Scientific Publishing Co. Pte. Ltd., Singapore, 1996)

[9] Conwell, E.: ‘Properties of silicon and germanium: II’, *Proc. IRE*, 1958, **46**, (6), pp. 1281–1300

[10] Choyke, W.J., Pensl, G.: ‘Physical properties of SiC’, *MRS Bull.*, 1997, **22**, (3), pp. 25–29

[11] Sze, S.M., Ng, K.K.: ‘*Physics of semiconductor devices*’ (Wiley, USA, 2006)

[12] Debye, P.P., Conwell, E.M.: ‘Electrical properties of N-type germanium’, *Phys. Rev.*, 1954, **93**, (4), pp. 693–706

[13] Long, D., Myers, J.: ‘Ionized-impurity scattering mobility of electrons in silicon’, *Phys. Rev.*, 1959, **115**, (5), pp. 1107–1118

[14] Stillman, G.E., Wolfe, C.M., Dimmock, J.O.: ‘Hall coefficient factor for polar mode scattering in N-type GaAs’, *J. Phys. Chem. Solids*, 1970, **31**, (6), pp. 1199–1204

[15] Pensl, G., Choyke, W.J.: ‘Electrical and optical characterization of SiC’, *Phys. B*, 1993, **185**, (1–4), pp. 264–283

[16] Baliga, B.J.: ‘*Silicon carbide power devices*’ (World Scientific, USA, 2005)

[17] Hall, R.N.: ‘Electron–hole recombination in germanium’, *Phys. Rev.*, 1952, **87**, (2), pp. 387–387

[18] Shockley, W., Read, W.T.: ‘Statistics of the recombinations of holes and electrons’, *Phys. Rev.*, 1952, **87**, (5), pp. 835–842

[19] Sah, C., Noyce, R., Shockley, W.: ‘Carrier generation and recombination in P–N junctions and P–N junction characteristics’, *Proc. IRE*, 1957, **45**, (9), pp. 1228–1243

[20] Long, D.: ‘Scattering of conduction electrons by lattice vibrations in silicon’, *Phys. Rev.*, 1960, **120**, (6), pp. 2024–2032

[21] Cheng, L., Snakin, I., Merrett, J.N., *et al.*: ‘Cryogenic and high temperature performance of 4H-SiC vertical junction field effect transistors (VJFETs) for space applications’. Proc. ISPSD ‘05. The 17th Int. Symp. on Power Semiconductor Devices and ICs, 2005, pp. 231–234

[22] Chen, S., Cai, C., Wang, T., *et al.*: ‘Cryogenic and high temperature performance of 4HSiC power MOSFETs’. 2013 Twenty-Eighth Annual IEEE Applied Power Electronics Conf. and Exposition (APEC), March 2013, pp. 207–210

[23] Pearson, G.L., Bardeen, J.: ‘Electrical properties of pure silicon and silicon alloys containing boron and phosphorus’, *Phys. Rev.*, 1949, **75**, (5), pp. 865–883

[24] Fritzsche, H.: ‘Resistivity and Hall coefficient of antimony-doped germanium at low temperatures’, *J. Phys. Chem. Solids*, 1958, **6**, (1), pp. 69–80

[25] Whitaker, J., Bolger, D.E.: ‘Shallow donor levels and high mobility in epitaxial gallium arsenide’, *Solid State Commun.*, 1966, **4**, (4), pp. 181–184

[26] Blakemore, J.S., Brown, W.J., Stass, M.L., *et al.*: ‘Thermal activation energy of manganese acceptors in gallium arsenide as a function of impurity spacing’, *J. Appl. Phys.*, 1973, **44**, (7), pp. 3352–3354

[27] Laube, M., Schmid, F., Pensl, G., *et al.*: ‘Electrical activation of high concentrations of N^+ and P^+ ions implanted into 4H-SiC’, *J. Appl. Phys.*, 2002, **92**, (1), pp. 549–554

[28] Negoro, Y., Kimoto, T., Matsunami, H., *et al.*: ‘Electrical activation of high-concentration aluminum implanted in 4H-SiC’, *J. Appl. Phys.*, 2004, **96**, (9), pp. 4916–4922

[29] Sreelakshmi, K., Satyam, M.: ‘Estimation of low temperature characteristics of JFETs from their room-temperature characteristics’, *Cryogenics*, 1996, **36**, (5), pp. 325–331

[30] van Roosbroeck, W., Shockley, W.: ‘Photon-radiative recombination of electrons and holes in germanium’, *Phys. Rev.*, 1954, **94**, (6), pp. 1558–1560

This is an open access article published by the IET under the Creative Commons Attribution License (http://creativecommons.org/licenses/by/3.0/)

[31] Haynes, J.R., Westphal, W.C.: 'Radiation resulting from recombination of holes and electrons in silicon', *Phys. Rev.*, 1956, **101**, (6), pp. 1676–1678
[32] Bemski, G.: 'Recombination properties of gold in silicon', *Phys. Rev.*, 1958, **111**, (6), pp. 1515–1518
[33] Iwata, H., Itoh, K.M.: 'Donor and acceptor concentration dependence of the electron Hall mobility and the Hall scattering factor in N-type 4H- and 6H-SiC', *J. Appl. Phys.*, 2001, **89**, (11), pp. 6228–6234
[34] Li, S.S., Thurder, W.R.: 'The dopant density and temperature dependence of electron mobility and resistivity in N-type silicon', *Solid-State Electron.*, 1977, **20**, (7), pp. 609–616
[35] Norton, P., Braggins, T., Levinstein, H.: 'Impurity and lattice scattering parameters as determined from Hall and mobility analysis in N-type silicon', *Phys. Rev. B*, 1973, **8**, (12), pp. 5632–5653
[36] Koenig, S.H., Brown, R.D., Schillinger, W.: 'Electrical conduction in N-type germanium at low temperatures', *Phys. Rev.*, 1962, **128**, (4), pp. 1668–1696
[37] Wolfe, C.M.: 'Electron mobility in high-purity GaAs', *J. Appl. Phys.*, 1970, **41**, (7), pp. 3088–3091
[38] Koizumi, A., Suda, J., Kimoto, T.: 'Temperature and doping dependencies of electrical properties in Al doped 4H-SiC epitaxial layers', *J. Appl. Phys.*, 2009, **106**, (1), p. 013716
[39] Erginsoy, C.: 'Neutral impurity scattering in semiconductors', *Phys. Rev.*, 1950, **79**, (6), pp. 1013–1014
[40] Harris, G.L.: '*Properties of silicon carbide*' (The IET, UK, 1995), vol. **93**
[41] Johnson, N.M., Moyer, M.D.: 'Absence of oxygen diffusion during hydrogen passivation of shallow acceptor impurities in single crystal silicon', *Appl. Phys. Lett.*, 1985, **46**, (1985), pp. 787–789
[42] Gali, A., Heringer, D., Deák, P., *et al.*: 'Isolated oxygen defects in 3C- and 4H-SiC: a theoretical study', *Phys. Rev. B*, 2002, **66**, (12), p. 125208
[43] Schmidt, J., Bothe, K.: 'Structure and transformation of the metastable boron- and oxygen-related defect center in crystalline silicon', *Phys. Rev. B*, 2004, **69**, (2), p. 024107

This is an open access article published by the IET under the Creative Commons Attribution License
(http://creativecommons.org/licenses/by/3.0/)